Arabidopsis Myosin XI: A Motor Rules the Tracks[1][C][W][OPEN]

Chao Cai, Jessica L. Henty-Ridilla, Daniel B. Szymanski, and Christopher J. Staiger*

Department of Biological Sciences (C.C., J.L.H.-R., C.J.S.), Center for the Direct Catalytic Conversion of Biomass to Biofuels (C.C., J.L.H.-R., D.B.S., C.J.S.), and Department of Agronomy (D.B.S.), Purdue University, West Lafayette, Indiana 47907

Plant cell expansion relies on intracellular trafficking of vesicles and macromolecules, which requires myosin motors and a dynamic actin network. Arabidopsis (*Arabidopsis thaliana*) myosin XI powers the motility of diverse cellular organelles, including endoplasmic reticulum, Golgi, endomembrane vesicles, peroxisomes, and mitochondria. Several recent studies show that there are changes in actin organization and dynamics in *myosin xi* mutants, indicating that motors influence the molecular tracks they use for transport. However, the mechanism by which actin organization and dynamics are regulated by myosin XI awaits further detailed investigation. Here, using high spatiotemporal imaging of living cells, we quantitatively assessed the architecture and dynamic behavior of cortical actin arrays in a mutant with three *Myosin XI* (*XI-1*, *XI-2*, and *XI-K*) genes knocked out (*xi3KO*). In addition to apparent reduction of organ and cell size, the mutant showed less dense and more bundled actin filament arrays in epidermal cells. Furthermore, the overall actin dynamicity was significantly inhibited in the *xi3KO* mutant. Because cytoskeletal remodeling is contributed mainly by filament assembly/disassembly and translocation/buckling, we also examined the dynamic behavior of individual actin filaments. We found that the *xi3KO* mutant had significantly decreased actin turnover, with a 2-fold reduction in filament severing frequency. Moreover, quantitative analysis of filament shape change over time revealed that myosin XI generates the force for buckling and straightening of both single actin filaments and actin bundles. Thus, our data provide genetic evidence that three Arabidopsis class XI myosins contribute to actin remodeling by stimulating turnover and generating the force for filament shape change.

Active transport is an important mechanism for eukaryotic cells to maintain the proper distribution of organelles and macromolecules and to deliver materials to sites of polar growth. Unlike animal cells, which use microtubules as tracks for long-distance transport, plants use predominantly actin filaments and myosin motors for vesicle trafficking and organelle positioning (Schuh, 2011). Studies using dominant-negative, RNAi, and knockout mutants indicate that the plant class XI myosins are motor molecules involved in transport of organelles, such as endoplasmic reticulum, Golgi, mitochondria, and peroxisomes (Avisar et al., 2008, 2009; Peremyslov et al., 2008, 2010; Prokhnevsky et al., 2008; Sparkes et al., 2008).

In addition to myosin XI, a functional network of dynamic actin filaments is critical for vesicle trafficking. Actin filaments or bundles provide the tracks for myosins to processively translocate using the energy of ATP hydrolysis. In Arabidopsis (*Arabidopsis thaliana*) epidermal cells, cortical actin filament arrays undergo continuous and rapid remodeling (Staiger et al., 2009; Smertenko et al., 2010). Two main features contribute to this dynamic rearrangement of actin filaments: translocation and buckling, and rapid assembly and disassembly (Staiger et al., 2009; Henty-Ridilla et al., 2013). The organization and dynamic behavior of actin filaments are regulated by a plethora of actin-binding proteins (Henty-Ridilla et al., 2013). Myosin is both a motor that drives long-distance cargo motility and also an actin regulator. In vitro biochemical assays show that skeletal muscle myosin II can induce the disassembly and fragmentation of actin filaments (Murrell and Gardel, 2012; Vogel et al., 2013). In budding yeast (*Saccharomyces cerevisiae*), myosin V is involved in the rapid translocation of actin cables and is responsible for the delivery of formin regulators, which affects the assembly of actin filaments at specific subcellular locations (Chesarone-Cataldo et al., 2011; Yu et al., 2011). By contrast, our understanding of how plant myosins are involved in the regulation of actin filament turnover and translocation is incomplete.

Studies on the effects of myosin on actin organization and dynamics in plant cells were initially performed by applying the drug 2,3-butanedione monoxime (BDM), which inhibits ATP hydrolysis by the myosin II head domain (Herrmann et al., 1992). For example, treatment with BDM alters actin organization in tip-growing root

[1] This work was supported by the Center for Direct Catalytic Conversion of Biomass to Biofuels, an Energy Frontier Research Center funded by the U.S. Department of Energy, Office of Science, Basic Energy Sciences (award no. DE–SC0000997).

* Address correspondence to staiger@purdue.edu.

The author responsible for distribution of materials integral to the findings presented in this article in accordance with the policy described in the Instructions for Authors (www.plantphysiol.org) is: Christopher J. Staiger (staiger@purdue.edu).

[C] Some figures in this article are displayed in color online but in black and white in the print edition.

[W] The online version of this article contains Web-only data.

[OPEN] Articles can be viewed online without a subscription.

www.plantphysiol.org/cgi/doi/10.1104/pp.114.244335

Downloaded from on November 28, 2017 - Published by www.plantphysiol.org
Copyright © 2014 American Society of Plant Biologists. All rights reserved.

hairs and pollen tubes (Tominaga et al., 2000; Zheng et al., 2009), as well as in cells of the root transition zone (Šamaj et al., 2000). A detailed description of the dynamic behavior of individual actin filaments in epidermal cells shows that BDM inhibits the turnover and shape change of actin filaments (Staiger et al., 2009). Although there is evidence that BDM can inhibit the motility of plant myosin XI in vitro (Tominaga et al., 2000; Funaki et al., 2004), this drug is typically applied at millimolar concentrations and probably does not inhibit all myosin-dependent cellular processes in plant cells (McCurdy, 1999). Therefore, genetic approaches using knockout mutants are important to interrogate the function of plant myosins. In Arabidopsis, actin filament bundles are oriented more transversely in *myosin xi* double, triple, and quadruple mutants compared with the predominantly longitudinal orientation in wild-type cells (Peremyslov et al., 2010; Ueda et al., 2010). Moreover, overall actin dynamics are reduced in root hairs of a *myosin xi-k* mutant (Park and Nebenführ, 2013). Also, actin filament arrays appear more randomized in tip-growing *Physcomitrella patens* protonemal cells when both *myosin xi* genes are knocked down (Vidali et al., 2010). Surprisingly, the overall dynamicity of the actin network is not altered in *Myosin XI* knockdown protonemal cells (Vidali et al., 2010). To gain a better understanding of the mechanism by which myosins impact actin filament organization and dynamics in plant cells, detailed analyses of actin filament properties in *myosin* mutants are necessary.

Here, we used a previously characterized *myosin xi-1*, *xi-2*, and *xi-k* triple knockout mutant (Peremyslov et al., 2010), combined with advanced live-cell imaging, to dissect how Arabidopsis myosin XI is involved in actin remodeling. With the high temporal and spatial resolution afforded by variable-angle epifluorescence microscopy (VAEM) and a set of metrics for analyzing filament dynamics, we found that the three class XI myosins generate force for the buckling and straightening of actin filaments and bundles, as well as promote actin filament turnover.

RESULTS

The Growth of Arabidopsis Seedlings Is Inhibited in a *myosin xi* Triple Knockout Mutant

Recently, it was reported that the velocity of myosin-dependent motility correlates with plant size, and knockout mutants of Arabidopsis *myosins* exhibit reduced organ size (Peremyslov et al., 2010; Tominaga et al., 2013). We analyzed the function of myosin XI in Arabidopsis seedlings using a previously characterized triple mutant line with *myosin xi-1*, *myosin xi-2*, and *myosin xi-k* knocked out (*xi3KO*; Peremyslov et al., 2010). To confirm that the loss of multiple myosin XI isoforms affected the expansion of organs, etiolated hypocotyls of the *xi3KO* mutant were examined. Organ length was significantly reduced in hypocotyls of *xi3KO* mutant seedlings compared with the wild type over a developmental time series (Fig. 1, A and B). We also examined light-grown roots. The length of roots from *xi3KO* seedlings was significantly reduced compared with the wild type (Fig. 1, C and D), which is consistent with a previous study (Peremyslov et al., 2010).

To test whether the reduction of organ length in the *xi3KO* mutant is due to inhibition of cell expansion, the length of epidermal cells from hypocotyls and the root elongation zone was measured. The growth of Arabidopsis hypocotyl epidermal cells occurs along a gradient, with cells at the base (near the root) finishing axial expansion earlier than those near the apex (near the cotyledons; Gendreau et al., 1997). The length and width of epidermal cells from both apical and basal regions of 5-d-old hypocotyls were significantly reduced in the *xi3KO* mutant (Fig. 1, E and F). Similarly, epidermal cells from the root elongation zone exhibited reduced length and width in the *xi3KO* mutant compared with the wild type (Fig. 1, G and H). These results suggest that loss of myosin XI inhibited cell and organ expansion in the early developmental stage.

The Architecture of Cortical Actin Arrays Is Altered in Epidermal Cells of the *xi3KO* Mutant

Myosins may have the ability to generate force on a preexisting actin network (Szymanski and Cosgrove, 2009) and Arabidopsis class XI myosins are reportedly involved in regulating actin organization (Peremyslov et al., 2010; Ueda et al., 2010). In *myosin xi* double, triple, and quadruple mutants, actin bundles appear to be more transversely oriented compared with the longitudinal orientation in wild-type cells (Peremyslov et al., 2010; Ueda et al., 2010). To further test whether the loss of myosin XI affects actin organization, we examined the cortical actin arrays in Arabidopsis seedlings expressing the yellow fluorescent protein fused with the second actin-binding domain from Arabidopsis FIMBRIN1 (YFP-fABD2) with VAEM. Representative images of epidermal cells from *xi3KO* hypocotyls showed that the cortical actin array was much less dense and more bundled compared with wild-type cells (Fig. 2A). Quantitative analyses were performed to analyze the architecture of cortical actin arrays. Two parameters, skewness and density, were measured to evaluate the extent of bundling and the percentage of occupancy of actin filaments in epidermal cells (Higaki et al., 2010; Henty et al., 2011; Li et al., 2012). The *xi3KO* mutant had a significantly reduced percentage of occupancy and increased bundling of actin arrays in both the apical and basal regions of the hypocotyl (Fig. 2, B and C). We also examined the angle of actin filaments with respect to the longitudinal axis of the cell, as well as the parallelness of actin filaments with respect to each other, using the methods of Ueda et al. (2010). The *xi3KO* mutant had a significantly increased angle in both apical and basal regions

Downloaded from on November 28, 2017 - Published by www.plantphysiol.org
Copyright © 2014 American Society of Plant Biologists. All rights reserved.

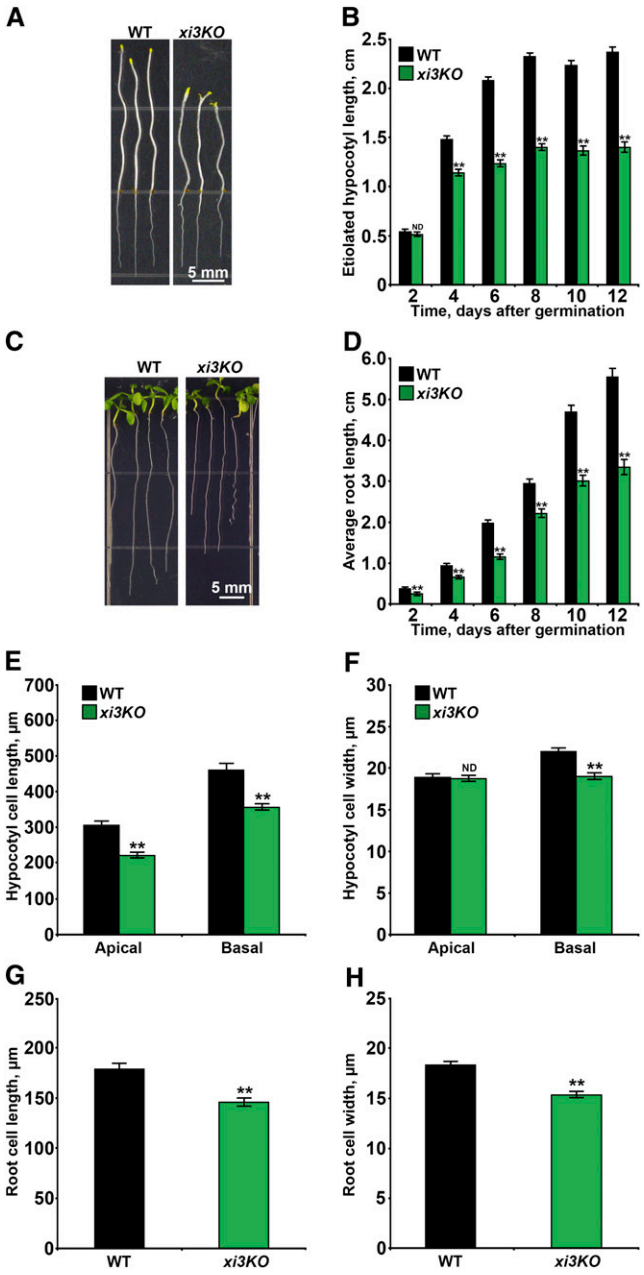

Figure 1. The myosin *xi3KO* mutant has reduced hypocotyl, root, and epidermal cell length. A, Representative examples of etiolated Arabidopsis seedlings from 5-d-old *myosin xi-1, xi-2, xi-k* triple knockout (*xi3KO*) mutant and the wild type (WT) are shown. Bar = 5 mm. B, The length of etiolated hypocotyls was significantly reduced in the *xi3KO* mutant compared with the wild type. Measurements were taken on alternate days for 12 d total. Values are means ± SE ($n \geq 50$ hypocotyls per genotype; Student's *t* test, $^{**}P < 0.01$). C, Representative examples of light-grown seedlings from 7-d-old *xi3KO* mutant and the wild type are shown. Bar = 5 mm. D, The length of light-grown roots was significantly reduced in the *xi3KO* mutant compared with the wild type. Measurements were performed on alternate days. Values are means ± SE ($n \geq 50$ roots per genotype; Student's *t* test, $^{**}P < 0.01$). E, The length of epidermal cells was measured at the apex (near cotyledons) and base (near root) of 5-d-old etiolated hypocotyls. The *xi3KO* mutant had significantly reduced epidermal cell length at both apex and base of the hypocotyl. Values are means ± SE ($n > 70$ cells from at least 10 hypocotyls per genotype; Student's *t* test, $^{**}P < 0.01$). F, The width of epidermal cells was measured at the apex and base of the same hypocotyls in E. The *xi3KO* mutant had significantly reduced epidermal cell width at the basal region of the hypocotyl. Values are means ± SE ($n > 100$ cells from at least 10 hypocotyls per genotype; Student's *t* test, $^{**}P < 0.01$). G, The length of epidermal cells was measured from the elongation zone of 10-d-old light-grown roots. The *xi3KO* mutant had significantly reduced epidermal cell length. Values are means ± SE ($n > 80$ cells from at least 10 roots per genotype; Student's *t* test, $^{**}P < 0.01$). H, The width of epidermal cells was measured at the elongation zone of the same roots in G. The *xi3KO* mutant had significantly reduced epidermal cell width. Values are means ± SE ($n > 100$ cells from at least 10 roots per genotype Student's *t* test, $^{**}P < 0.01$). ND, No significant difference.

of the hypocotyl (Fig. 2D) and significantly reduced filament-filament parallelness in the basal region of the hypocotyl (Fig. 2E), suggesting that actin filament arrays in the *xi3KO* mutant are more transversely oriented and disorganized.

To examine whether the change in architecture of actin arrays is apparent in other organs, the extent of bundling and the percentage of occupancy of actin filaments were also evaluated in light-grown roots of the *xi3KO* mutant. The actin arrays were more bundled and less dense in epidermal cells from the root elongation zone (Fig. 3, A–C), which is consistent with the result in hypocotyls. We also examined overall filament orientation and filament parallelness in root epidermal cells. The actin filament arrays showed an increase of both angle and parallelness in epidermal cells from the root elongation zone (Fig. 3, D and E). Collectively, these results demonstrate that the three class XI myosins are involved in regulation of actin organization.

Cortical Actin Array Dynamics in Epidermal Cells Are Reduced in the *xi3KO* Mutant

Cortical actin arrays in Arabidopsis hypocotyl epidermal cells undergo constant remodeling and filament turnover (Staiger et al., 2009; Smertenko et al., 2010). It has been reported that knocking down *Myosin XI* in *Physcomitrella patens* protonemal cells does not affect the overall dynamics of actin organization (Vidali et al., 2010). To analyze whether the overall dynamicity of cortical actin arrays is altered in Arabidopsis when three *Myosin XI* genes are knocked out, time-lapse VAEM series were collected from epidermal cells of etiolated hypocotyls expressing YFP-fABD2. Actin arrays in the epidermal cells from the *xi3KO* mutant appeared to be much less dynamic when compared with wild-type cells at both apical and basal regions of the hypocotyl (Fig. 4A). To quantify global actin dynamics, a correlation coefficient analysis was performed (Vidali et al., 2010). This analysis was accomplished by calculating pixel intensity correlation for all pairwise temporal intervals from multiple time-lapse series. The overall

Downloaded from on November 28, 2017 - Published by www.plantphysiol.org
Copyright © 2014 American Society of Plant Biologists. All rights reserved.

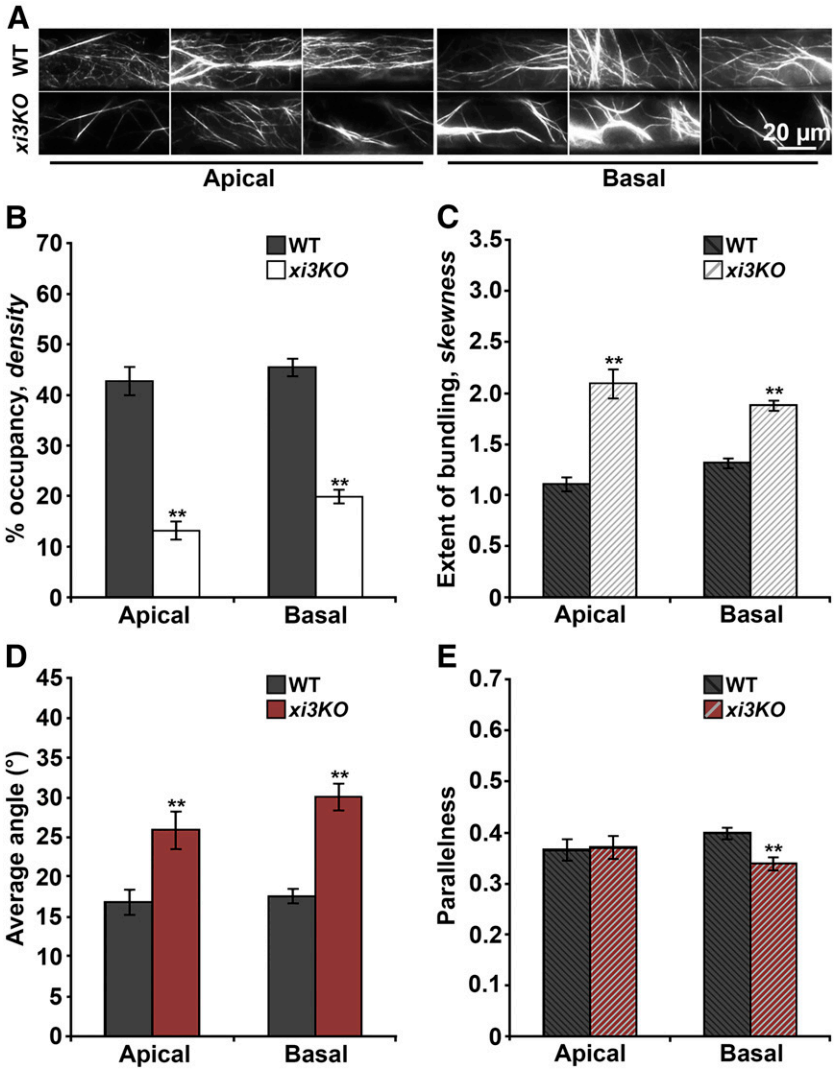

Figure 2. The architecture of actin arrays in epidermal cells of the *xi3KO* mutant is altered. A, Representative images of epidermal cells from 5-d-old dark-grown hypocotyls of wild-type (WT) and *xi3KO* seedlings expressing YFP-fABD2. VAEM images were collected from the apical and basal regions of the hypocotyl. Bar = 20 μm. B and C, Quantitative analyses of the architecture of cortical actin arrays in wild-type and *xi3KO* mutant epidermal cells. B, Percentage of occupancy (density) was measured. Filament density was significantly decreased in epidermal cells at both apical and basal regions of hypocotyls in the *xi3KO* mutant compared with the wild type. Values given are means ± SE ($n \geq 150$ images from 30 hypocotyls per genotype; Student's *t* test, $^{**}P < 0.01$). C, The extent of filament bundling (skewness) was measured. Bundling was significantly increased in epidermal cells at both apical and basal regions of the hypocotyl in *xi3KO*. The same images used for B were analyzed for bundling (Student's *t* test, $^{**}P < 0.01$). D and E, Quantitative analyses of the orientation of cortical actin arrays in wild-type and *xi3KO* mutant epidermal cells. D, Average angle of actin filaments with respect to the longitudinal axis of epidermal cells was measured. Angle was significantly increased in epidermal cells at both apical and basal regions of hypocotyls in the *xi3KO* mutant compared with the wild type. Values given are means ± SE (Student's *t* test, $^{**}P < 0.01$). E, The parallelness of actin filaments with respect to each other was measured. Parallelness was significantly reduced in epidermal cells at the basal regions of the hypocotyl in *xi3KO* compared with the wild type. The same images used for B and C were analyzed for angle and parallelness (Student's *t* test, $^{**}P < 0.01$).

actin dynamics is reflected by the rate of decay of correlation coefficient values as a function of time interval. A faster decay of the curve suggests more active actin dynamics. The correlation coefficient curve for the *xi3KO* mutant decayed significantly slower compared with the wild type (Fig. 4, B and C), indicating decreased dynamics of the actin arrays in *xi3KO* mutant cells. Both apical and basal regions of the dark-grown hypocotyl showed a reduction in actin dynamicity, indicating that myosin XI regulates actin dynamics at different developmental stages. Moreover, we measured the overall dynamicity for different subpopulations of actin filaments. The correlation coefficient curves for both single actin filaments and actin bundles decayed significantly slower in the *xi3KO* mutant compared with the wild type (Supplemental Fig. S1, C–F; Supplemental Methods S1), indicating that these three myosins XI are involved in regulating the dynamics of both single actin filament and actin bundles. We also applied BDM, a myosin ATPase inhibitor, on hypocotyl epidermal cells expressing GFP-fABD2. The correlation coefficient curves decayed significantly slower and in a dose-dependent manner after 5-min treatments with different concentrations of BDM (Fig. 4, D and E), thus phenocopying the *xi3KO* mutant.

To test whether the reduction of overall dynamics in *xi3KO* occurs in other organs and developmental states, we examined the correlation coefficient of time-lapse images collected from epidermal cells in the elongation zone of light-grown roots. The results show that the overall dynamicity of actin arrays in *xi3KO* root epidermal cells was reduced compared with the wild type (Fig. 3F), which is consistent with the result from hypocotyls. Collectively, these data indicate that three Arabidopsis myosin XI isoforms are involved in promoting the overall dynamicity of actin filament arrays.

The Dynamic Properties of Single Actin Filaments Are Altered in the *xi3KO* Mutant

Two main features contribute to the dynamic behavior of actin filaments in the cortical array of epidermal

Downloaded from on November 28, 2017 - Published by www.plantphysiol.org
Copyright © 2014 American Society of Plant Biologists. All rights reserved.

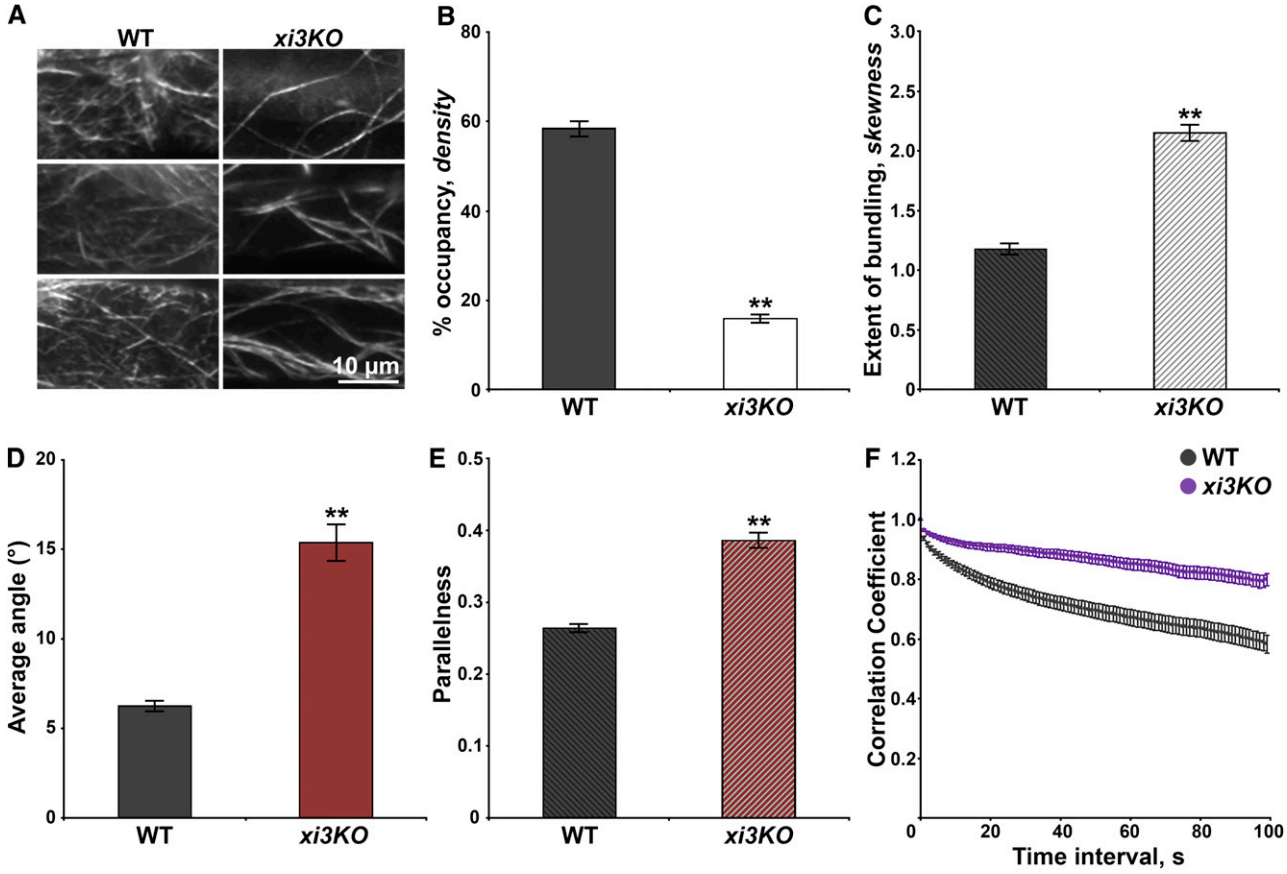

Figure 3. The architecture and overall dynamicity of actin arrays in epidermal cells from the root elongation zone of the *xi3KO* mutant are changed. A, Representative images of epidermal cells from 7-d-old light-grown roots of wild-type (WT) and *xi3KO* seedlings expressing YFP-fABD2. VAEM images were collected from the elongation zone of the root. Bar = 10 μm. B and C, Quantitative analyses of the architecture of actin arrays in wild-type and *xi3KO* mutant epidermal cells. B, Percentage of occupancy (density) was measured. Filament density was significantly decreased in the *xi3KO* mutant compared with the wild type. Values given are means ± SE ($n \geq 100$ images from 30 seedlings per genotype; Student's *t* test, $^{**}P < 0.01$). C, The extent of filament bundling (skewness) was measured. Bundling was significantly increased in the *xi3KO* mutant compared with the wild type. The same images used for B were analyzed for bundling (Student's *t* test, $^{**}P < 0.01$). D and E, Quantitative analyses of the orientation of cortical actin arrays in wild-type and *xi3KO* mutant epidermal cells. D, Average angle of actin filaments with respect to the longitudinal axis of epidermal cells was measured. Angle was significantly increased in the *xi3KO* mutant compared with the wild type. Values given are means ± SE (Student's *t* test, $^{**}P < 0.01$). E, The parallelness of actin filaments with respect to each other was measured. Parallelness was significantly increased in *xi3KO* compared with the wild type. The same images used for B and C were analyzed for angle and parallelness (Student's *t* test, $^{**}P < 0.01$). F, Pairwise correlation coefficient was calculated at all possible temporal spacings from time-lapse series of epidermal cells in the elongation zone of the root. Filaments in *xi3KO* had significantly reduced overall actin dynamicity compared with the wild type. Values given are means ± SE ($n \geq 35$ cells from 15 seedlings per genotype; ANOVA, $P < 0.01$).

cells: filament translocation and buckling, and filament turnover by assembly and disassembly events (Staiger et al., 2009; Smertenko et al., 2010; Henty-Ridilla et al., 2013). To dissect the mechanisms through which Arabidopsis myosin XI regulates actin rearrangements, we tracked the dynamic behavior of single actin filaments in time-lapse VAEM series collected from hypocotyl epidermal cells (Staiger et al., 2009).

An in vitro reconstituted system was used to show that skeletal muscle myosin II could induce the disassembly and fragmentation of actin filaments (Murrell and Gardel, 2012; Vogel et al., 2013). We hypothesize that the loss of myosin XI would cause a decrease in actin turnover in Arabidopsis epidermal cells. As shown in Table I, actin filaments in *xi3KO* mutant cells showed a decrease in severing frequency to about one-half of the wild-type level, as well as a 50% increase in maximum filament length and an almost 2-fold increase in maximum filament lifetime. These results demonstrate that actin turnover was reduced in the *xi3KO* mutant, because in Arabidopsis epidermal cells, actin filament disassembly is mainly achieved through severing activity (Staiger et al., 2009; Henty et al., 2011).

Downloaded from on November 28, 2017 - Published by www.plantphysiol.org
Copyright © 2014 American Society of Plant Biologists. All rights reserved.

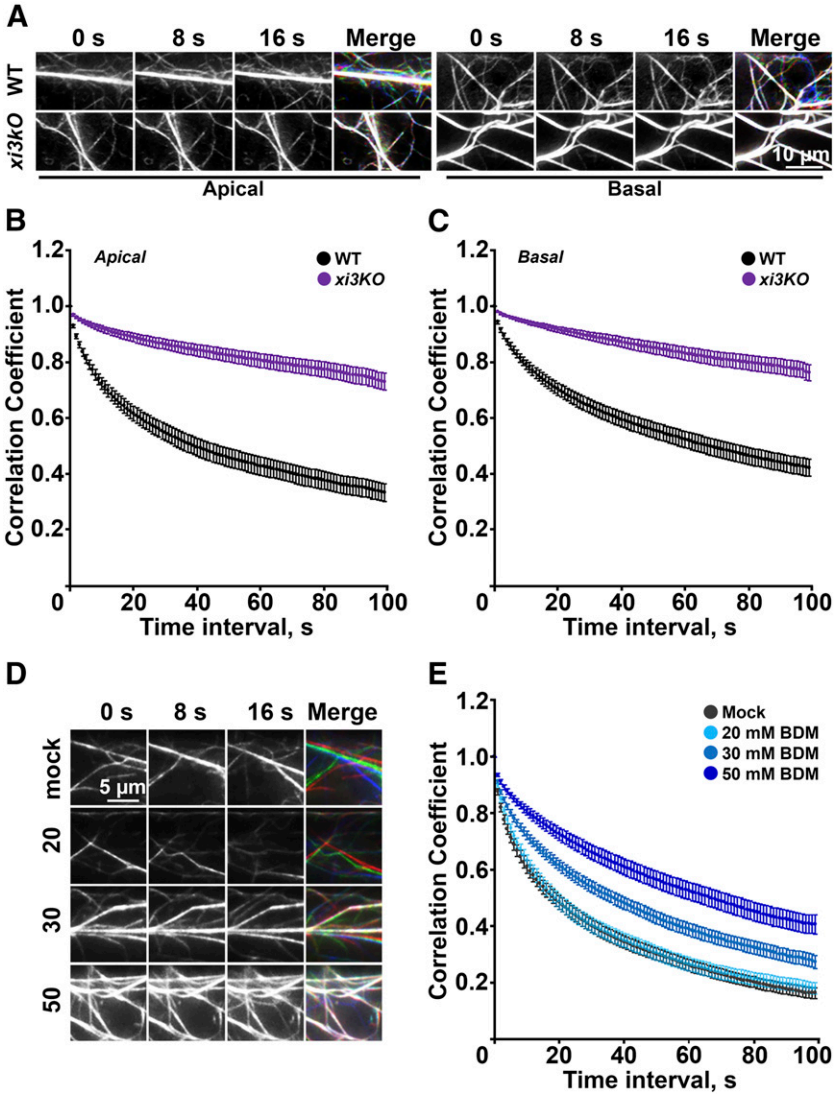

Figure 4. Overall actin dynamicity is reduced in the *xi3KO* mutant and BDM-treated epidermal cells. A, Representative time-lapse VAEM images taken from 5-d-old dark-grown hypocotyls of wild-type (WT) and *xi3KO* Arabidopsis seedlings expressing YFP-fABD2. Images shown were taken from epidermal cells in the apical and basal regions of the hypocotyl and displayed at 8-s intervals. The merged image shows the three time points in separate colors (red, green, and blue). Bar = 10 μm. B and C, Pairwise correlation coefficient was calculated at all possible temporal spacings from time-lapse series collected at the apical (B) and basal (C) regions of the hypocotyl. Filaments in *xi3KO* had reduced overall actin dynamicity compared with the wild type. Values given are means ± SE ($n \geq 40$ cells from 10 seedlings per genotype; ANOVA, $P < 0.01$). D, Representative time-lapse VAEM images taken from 5-d-old dark-grown hypocotyls treated with 0 (mock), 20, 30, or 50 mM BDM for 5 min. Images shown were taken from epidermal cells in the basal region of the hypocotyl and displayed at 8-s intervals. Bar = 5 μm. E, Pairwise correlation coefficient was calculated at all possible temporal spacings from time-lapse series collected at the basal region of the hypocotyl. Epidermal cells showed a dose-dependent reduction in overall actin dynamicity. Values given are means ± SE ($n \geq 40$ cells from 10 seedlings per genotype; ANOVA, $P < 0.01$).

In budding yeast, mutation of myosin V causes an apparent reduction in actin cable extension rates, which results from the loss of filament populations that translocated at rates greater than 2 μm s^{-1} (Yu et al., 2011). Given that myosin XI in Arabidopsis is a close relative of yeast myosin V (Hodge and Cope, 2000), we hypothesize that the average filament elongation rate in *xi3KO* would be reduced due to the loss of fast-growing filaments, assuming that filaments with fast elongation rates are actually translocating rather than assembling from monomers. By tracking the behavior of dynamic filament ends, however, no significant change of average filament elongation rate was detected between *xi3KO* and wild-type control cells (Table I; Fig. 5A). We further categorized the filaments into three populations based on elongation rate, as described in Yu et al. (2011). As shown in Figure 5B, the proportion of filaments with different elongation rates was not altered in *xi3KO* compared with the wild type. Unlike the situation in the budding yeast, the fastest population of growing filament ends (>2 μm s^{-1}) remained the same statistically as the wild-type control. Because the actin cable extension measured in Yu et al. (2011) is a combination of elongation and translocation, these results indicate that we probably measured different aspects of actin dynamics from those in yeast. Our results show that these three class XI Arabidopsis myosins are not involved in the regulation of actin assembly.

We also quantified several other single actin filament dynamic parameters to determine whether myosin XI regulates additional aspects of the dynamic behavior, for example, the availability of filament ends (Table I). The regrowth frequency, annealing frequency, and filament origin were not significantly different in *xi3KO* cells compared with the wild type. Collectively, these results indicate that the three class XI Arabidopsis myosins do not have a major effect on the behavior of dynamic filament ends. However, class XI myosins do contribute to filament disassembly through modulation

Downloaded from on November 28, 2017 - Published by www.plantphysiol.org
Copyright © 2014 American Society of Plant Biologists. All rights reserved.

Table I. *Comparison of actin dynamics parameters from wild-type and xi3KO epidermal cells*

Measurements taken from epidermal cells in 5-d-old hypocotyls of the *xi3KO* mutant and wild-type plants. Values given are means ± SE, with $n > 50$ filaments from $n > 10$ epidermal cells and at least 10 hypocotyls per line. ND, Not significantly different from the wild-type control value by Student's *t* test ($P > 0.05$). *Significantly different from the wild-type control value by Student's *t* test ($P < 0.05$). **Significantly different from the wild-type control value by Student's *t* test ($P < 0.001$). For filament origin, $n > 300$ filament from $n > 30$ epidermal cells and at least 10 hypocotyls per line. ‡, Not significantly different from the wild-type control value by ANOVA ($P > 0.05$).

Stochastic Dynamics Parameters	Wild Type	*xi3KO*
Apical		
Elongation rate ($\mu m\ s^{-1}$)	1.76 ± 0.04	1.78 ± 0.05ND
Filament breaks (breaks)	3.5 ± 0.1	3.8 ± 0.2ND
Severing frequency (breaks $\mu m^{-1}\ s^{-1}$)	0.016 ± 0.001	0.008 ± 0.001**
Max length (μm)	11.2 ± 0.4	15.0 ± 1.0**
Max lifetime (s)	21.1 ± 0.6	37.9 ± 1.8**
Regrowth of severed ends (%)	5.2 ± 1.7	3.3 ± 1.2ND
Annealing of severed ends (%)	3.8 ± 1.5	1.3 ± 0.7ND
Filament origin (% per cell)		
De novo	28.8 ± 3.5	27.5 ± 8.6‡
Ends	21.4 ± 3.9	20.9 ± 7.7‡
Side	49.2 ± 3.1	51.3 ± 5.4‡
Convolutedness	1.25 ± 0.05	1.11 ± 0.01*
Rate of change of convolutedness (s^{-1})	0.09 ± 0.01	0.04 ± 0.003**
Basal		
Elongation rate ($\mu m\ s^{-1}$)	1.79 ± 0.05	1.86 ± 0.05ND
Filament breaks (breaks)	4.7 ± 0.2	4.5 ± 0.2ND
Severing frequency (breaks $\mu m^{-1}\ s^{-1}$)	0.014 ± 0.001	0.007 ± 0.001**
Max length (μm)	12.6 ± 0.4	17.0 ± 0.7**
Max lifetime (s)	27.6 ± 0.8	44.1 ± 1.9**
Regrowth of severed ends (%)	3.3 ± 1.1	3.2 ± 1.2ND
Annealing of severed ends (%)	2.6 ± 1.1	1.2 ± 0.8ND
Filament origin (% per cell)		
De novo	29.5 ± 2.6	28.4 ± 7.1‡
Ends	21.0 ± 3.0	21.7 ± 6.5‡
Side	48.6 ± 3.4	50.6 ± 4.4‡
Convolutedness	1.27 ± 0.04	1.20 ± 0.04ND
Rate of change of convolutedness (s^{-1})	0.09 ± 0.01	0.03 ± 0.003**

of severing frequency, which was reduced 2-fold in the mutant cells.

Myosin XI Generates Force for Filament and Bundle Buckling and Straightening

Cortical actin filaments undergo continuous shape changes, as well as stochastic dynamic turnover (Staiger et al., 2009; Smertenko et al., 2010). It was shown in a previous study that BDM, a myosin ATPase inhibitor, could reduce actin dynamics by inhibiting filament buckling and straightening events (Staiger et al., 2009). To test whether myosin XI contributes to filament buckling and straightening, we examined the shape of actin filaments in VAEM time-lapse series collected from hypocotyl epidermal cells. Actin filaments in wild-type cells showed continuous buckling and straightening events (Fig. 6A, 24 and 30 s); however, in *xi3KO* mutant cells, the shape of actin filaments remained relatively constant (Fig. 6B). To quantitatively assess the shape of actin filaments, we measured convolutedness and the rate of change of convolutedness. Convolutedness is a dimensionless measure of the ratio of filament length divided by the distance of a straight line connecting the plus and minus ends (Smertenko et al., 2010; Fig. 6A). As shown in Figure 6C, the convolutedness of actin filaments showed a modest reduction (apical) or no difference (basal) in *xi3KO* epidermal cells compared with the wild type. However, the *xi3KO* mutant showed an approximately 2- to 3-fold reduction in the rate of change of convolutedness, indicating the filament buckling and straightening is reduced when three myosin XI isoforms are eliminated. We also examined these parameters for actin filament bundles. Similar to single actin filaments, bundles had a significantly reduced rate of change of convolutedness in the *xi3KO* mutant (Fig. 6, E and F). In sum, these results suggest that three class XI myosins regulate not the overall shape but the shape change of actin filaments and bundles.

DISCUSSION

In this study, we dissected the role of three Arabidopsis class XI myosins in organization and dynamics of cortical actin arrays using high spatiotemporal

Downloaded from on November 28, 2017 - Published by www.plantphysiol.org
Copyright © 2014 American Society of Plant Biologists. All rights reserved.

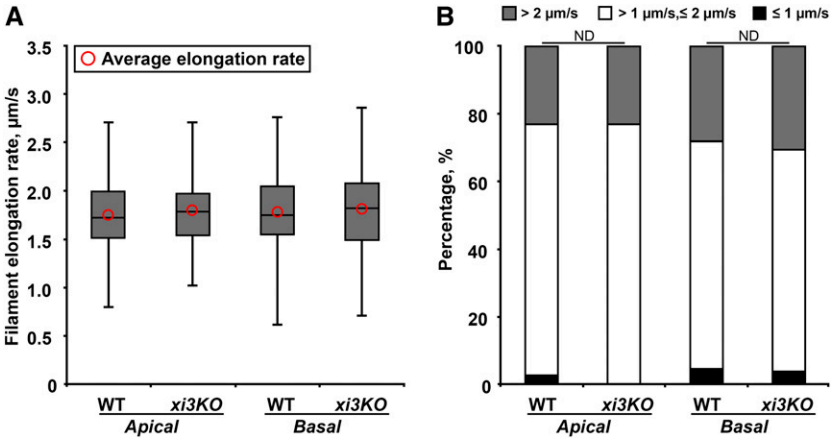

Figure 5. Elongation rate of growing filament ends is not altered in *xi3KO* mutant. A, Box plots show the elongation rate of growing actin filaments in the wild type (WT) and the *xi3KO* mutant. The box spans between the first and the third quartile. The line inside the box shows the median. The bars show the minimum and maximum values. Circles show the average filament elongation rates ($n > 100$ filaments per genotype). B, The elongation rate of growing filaments analyzed in A was binned into three populations: ≤ 1 μm s^{-1}, 1 to 2 μm s^{-1}, and >2 μm s^{-1}. The percentage of each population was calculated. ND indicates not significantly different from wild-type control by χ^2 test ($P > 0.05$). [See online article for color version of this figure.]

resolution imaging of living plant epidermal cells. Arabidopsis myosin XI is important for the expansion of organs and cells at different developmental stages. The *myosin xi-1*, *xi-2*, and *xi-k* triple mutant is a dwarf plant with significantly reduced etiolated hypocotyl length and light-grown root length, as shown previously (Peremyslov et al., 2010). Cell expansion was significantly inhibited in hypocotyls and roots of the *xi3KO* mutant. Moreover, the architecture of cortical actin filament arrays was less dense and more bundled in the *xi3KO* mutant compared with the wild type. These three class XI myosins also contribute to the overall dynamicity of actin in epidermal cells, which is significantly inhibited in the *xi3KO* mutant. This effect on dynamics of actin has two main features: myosin XI promotes the turnover of actin filaments by enhancing severing frequency, and it generates the force for buckling and straightening of single actin filaments and filament bundles. Finally, the three class XI myosins appear not to be involved in regulating the behavior of dynamic filament ends or filament assembly.

The regulation of actin organization by plant myosins has been observed in many studies; however, the results vary in different cell types and based on different methods for inhibiting myosin activity. BDM inhibits the ATPase activity of myosin head domain (Funaki et al., 2004), and its effect on actin filaments in plant cells varies depending on the dose and duration of treatment. Treatment of pollen tubes and root hairs with BDM for 1 h causes a loss of longitudinal orientation of actin bundles in the shank region (Tominaga et al., 2000), whereas short-term treatment (10 min) of growing root hairs with BDM induces the formation of fine actin filament arrays extending into the apical clear zone (Zheng et al., 2009). Due to apparent genetic redundancy within the large gene family, mutants that have multiple *myosin xi* genes knocked out were created to study their function in plant cells (Peremyslov et al., 2008, 2010; Prokhnevsky et al., 2008; Ueda et al., 2010; Ojangu et al., 2012). The Arabidopsis *myosin xi-k, xi-2* double mutant has randomized actin bundle arrays compared with the predominantly longitudinal orientation in wild-type epidermal cells (Ueda et al., 2010). The midvein epidermal cells in triple and quadruple mutants of Arabidopsis *myosin xi* (*xi-1, xi-2, xi-i, xi-k*) lose their longitudinal bundles, and actin filament arrays become more transversely oriented (Peremyslov et al., 2010). Similar to BDM treatment, the actin bundles protrude into the apical clear zone of root hairs in these triple and quadruple mutants (Peremyslov et al., 2010). In tip-growing *P. patens* protonemal cells, actin filament arrays lose their parallel longitudinal orientation and become more randomized when both *Myosin XI* genes are knocked down (Vidali et al., 2010). In this study, we examined the architecture and organization of cortical actin filament arrays in growing and nongrowing epidermal cells from different organs. With quantitative live-cell imaging, we found that the abundance of actin filaments in the cortical array was significantly reduced in the *xi3KO* mutant and that actin filaments were much more bundled compared with the wild type. Moreover, the cortical actin array is more transversely oriented and disorganized in the *xi3KO* mutant compared with the wild type.

In plant cells, actin filament arrays undergo rapid and continuous remodeling (Staiger et al., 2009; Vidali et al., 2009; Smertenko et al., 2010). Recent studies quantified this overall dynamicity of actin arrays to test whether plant myosin XI is involved in the regulation of actin dynamics; however, the results are not consistent between organisms. Knocking down both *Myosin XI* genes in *P. patens* protonemal cells has no effect on the overall actin dynamicity (Vidali et al., 2010), whereas root hairs of the Arabidopsis *myosin xi-k* mutant show a reduction of overall dynamicity of actin filament arrays (Park and Nebenführ, 2013). In this study, we demonstrated that three class XI myosins are important to maintain overall actin dynamicity in diffuse-growing epidermal cells of Arabidopsis. The overall actin dynamicity was significantly inhibited in the *xi3KO* mutant in both growing and nongrowing hypocotyl cells as well as in root elongation zone epidermal cells. In addition, we demonstrated that the myosin ATPase inhibitor BDM inhibits overall actin dynamicity.

Downloaded from on November 28, 2017 - Published by www.plantphysiol.org
Copyright © 2014 American Society of Plant Biologists. All rights reserved.

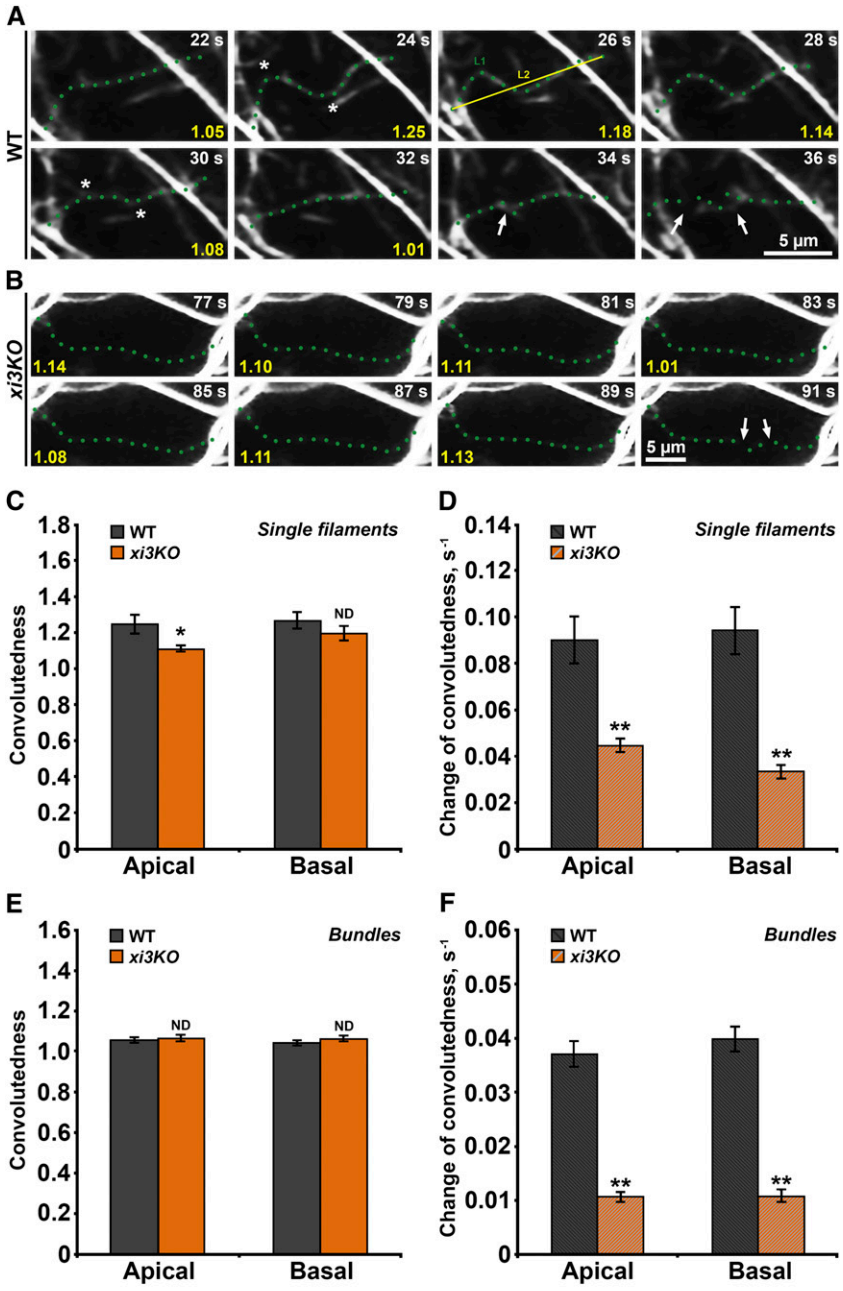

Figure 6. The rate of filament buckling and straightening is reduced in the *xi3KO* mutant. A and B, Time-lapse VAEM series show examples of actin filament buckling and straightening in wild-type (WT) epidermal cells (A) but not in the *xi3KO* mutant cells (B). The filament highlighted in A buckled (asterisks) at two sites at 24 s and straightened (asterisks) at 30 s and then got severed at 34 and 36 s (arrows). However, the filament highlighted in B showed no visible shape change during the entire time series and eventually got severed at 91 s (arrows). Bar = 5 μm. C and D, Quantitative analyses of single actin filament shape change in wild-type and *xi3KO* mutant epidermal cells. C, Convolutedness was measured as the ratio of filament length (L1) divided by the Euclidean distance (L2), as shown in A. Values for the representative filaments are stamped in yellow in A and B. Convolutedness showed a modest reduction at the apical region of the hypocotyl but no significant difference in *xi3KO* compared with the wild type at the base of hypocotyls ($n \geq 50$ filaments from 10 hypocotyls per genotype; Student's *t* test, $^{*}0.01 < P < 0.05$). D, Rate of change of convolutedness of single actin filaments was measured. The rate of change of convolutedness was significantly decreased in cells from both apical and basal regions of hypocotyls in the *xi3KO* mutant compared with the wild type. Values given are means ± SE. The same images used for C were analyzed for D (Student's *t* test, $^{**}P < 0.01$). E and F, Quantitative analyses of actin bundle shape change in wild-type and *xi3KO* mutant epidermal cells. E, Convolutedness of actin filament bundles showed no significant difference in *xi3KO* compared with the wild type at either the apical or basal region of hypocotyls ($n \geq 50$ bundles from 10 hypocotyls per genotype; Student's *t* test, $^{*}0.01 < P < 0.05$). F, The rate of change of convolutedness of actin filament bundles was significantly decreased in cells from both apical and basal regions of hypocotyls in the *xi3KO* mutant compared with the wild type. Values given are means ± SE. The same images used for E were analyzed for F (Student's *t* test, $^{**}P < 0.01$). ND, No significant difference.

The dynamic behavior of actin filament arrays is contributed mainly by two features: filament assembly and disassembly, and filament translocation and buckling (Henty-Ridilla et al., 2013; Li et al., 2014a). These properties of actin filaments can be tracked with high-resolution time-lapse imaging (Staiger et al., 2009). Previous data from diverse classes of myosin demonstrate that motors can regulate the dynamics of actin filaments. In budding yeast, myosin V delivers formin regulators, which locally alter the assembly of actin filaments at the bud neck (Chesarone-Cataldo et al., 2011). Further, yeast myosin V enhances actin cable motility by promoting translocation of bundles (Yu et al., 2011). Conventional myosin II from rabbit skeletal muscle is able to induce the fragmentation of actin filaments, which facilitates the turnover of actin in vitro (Murrell and Gardel, 2012; Vogel et al., 2013). Here, by tracking the dynamic behavior of individual actin filaments in vivo, we quantitatively assessed the effects of loss of myosin XI on parameters of stochastic turnover. We found that three Arabidopsis myosins XI are critical for the turnover of actin. In the *xi3KO* mutant, severing frequency was significantly inhibited compared with the wild type, which led to an increase in maximum filament length and lifetime. In this case, myosin might generate tension on filaments that facilitates the action

Downloaded from on November 28, 2017 - Published by www.plantphysiol.org
Copyright © 2014 American Society of Plant Biologists. All rights reserved.

of other severing proteins. Alternatively, filament buckling by myosin could directly result in breaks along the length of the polymer. Regardless of mechanism, this is the first genetic evidence that myosin is involved in regulating filament fragmentation and actin turnover in plant cells.

Myosin XI appears not to be involved in regulating filament ends or filament assembly in Arabidopsis epidermal cells. The *myosin xi3KO* mutant did not have altered annealing and regrowth frequencies, which indicates that the number of free filament ends was not changed. Actin filaments originate from different locations (de novo, side, and end), suggesting different mechanisms of nucleation (Staiger et al., 2009). The *xi3KO* mutant did not show any alteration to the proportion of filament origins compared with the wild type. More importantly, in budding yeast, the distribution of distinct populations of actin cables reveals different molecular mechanisms whereby barbed-end elongation is coordinated (Chesarone-Cataldo et al., 2011; Yu et al., 2011). Cable motility rates that are faster than 2 μm s^{-1} are due to filament translocation driven by the type V myosin Myo2p (Yu et al., 2011). Here, we found that there was no significant change in either the average or the distribution of elongation rates in the *xi3KO* mutant. These data indicate that the mechanistically distinct types of elongating barbed ends in plant epidermal cells (Li et al., 2014b) are not regulated by the three class XI myosins and also confirm that the dynamic behavior of filament ends is not regulated by the three class XI myosins.

Filament buckling and straightening is another important feature that contributes to the dynamics of actin filament arrays. A previous study using BDM showed that plant myosin may generate the force for buckling and straightening of actin filaments (Staiger et al., 2009). We hypothesize that myosin XI powers filament buckling by facilitating the sliding of antiparallel filaments past each other, by translocation of filaments along membranes, or both (Szymanski and Cosgrove, 2009; Staiger et al., 2009; Henty-Ridilla et al., 2013; Li et al., 2014a). Here, using a genetic approach, we confirmed that three class XI myosins contribute to the shape change of actin filaments. The rate of change of convolutedness was significantly reduced in epidermal cells of the *xi3KO* mutant. Moreover, although the thick actin bundles are less dynamic than single actin filaments (Staiger et al., 2009), the shape change of actin bundles was also inhibited in the *xi3KO* mutant. Thus, this is the first piece of evidence indicating that three class XI myosins generate force for not only single actin filaments, but also actin bundles in plant epidermal cells. Changes in filament and bundle shape could be powered by antiparallel filament sliding, trafficking of endomembrane compartments along actin filaments, translocation of filaments at the plasma membrane, bulk cytoplasmic streaming, or all of the above.

Plant cell expansion depends on the delivery of membranes and cell wall materials (Smith and Oppenheimer, 2005; Li et al., 2014a). One component of this delivery mechanism is cargo selection. For example, the trafficking of noncellulosic cell wall components is assumed to depend on actin and myosin (Nebenführ et al., 1999). Arabidopsis myosin XI facilitates the motility of secretory vesicles, and a novel cargo adaptor protein was recently identified (Peremyslov et al., 2012, 2013). The other key aspect in myosin-dependent secretion is actin track organization. Proper actin organization is important for the patterning and lifetime of cellulose synthase complex residency at the plasma membrane, which, in turn, impacts crystalline cellulose deposition (Sampathkumar et al., 2013). In this context, anchored myosin motors might generate forces on the actin bundles that support transvacuolar strands and create stable transport pathways to particular locations at the cortex (Szymanski and Cosgrove, 2009). Studying mutants of other conserved actin-binding proteins revealed a correlation between certain actin filament features and cell expansion (Smith and Oppenheimer, 2005; Hussey et al., 2006; Li et al., 2014a). It is hypothesized that longer filament length and increased lifetime enhance axial cell expansion by establishing more efficient tracks for vesicle trafficking (Henty-Ridilla et al., 2013; Li et al., 2014a, 2014b). Our data show that in the *xi3KO* mutant, filament length and lifetime were increased due to the inhibition of severing frequency. However, although filament length and lifetime are increased, cell length and width in the *xi3KO* mutant were reduced. This could suggest that myosin XI is downstream of actin length and lifetime in regulating cell expansion. In other words, track length and lifetime are not relevant when the motors and cargo delivery are inhibited. Moreover, a recent study shows that the velocity of myosin positively correlates with cell size by replacing the ATPase head domain with faster and slower motors (Tominaga et al., 2013). Such mutants provide a unique opportunity to study, in more detail, the relationship between myosin motor activity and actin tracks. For example, it should be possible to test whether the change of myosin velocity would affect turnover of actin filaments or whether a higher velocity of myosin would generate more force for filament buckling and straightening, or both.

MATERIALS AND METHODS

Plant Material and Growth Conditions

The Arabidopsis (*Arabidopsis thaliana*) *xi3KO* mutant and *xi3KO* mutant expressing vYFP-fABD2 were characterized previously (Peremyslov et al., 2010). Seeds were surface sterilized and stratified at 4°C for 3 d on one-half-strength Murashige and Skoog medium. For dark-grown hypocotyls, seedlings were grown on medium supplemented with 1% (w/v) Suc and 1% (w/v) agar. After 4 h of exposure to light, plates were wrapped in three layers of aluminum foil and placed in continuous darkness. For light-grown seedlings, seeds were plated on one-half-strength Murashige and Skoog medium supplemented with 0% (w/v) Suc and 0.6% (w/v) agar (Dyachok et al., 2011; Li et al., 2012). Seedlings were grown vertically under long-day conditions (16 h of light/8 h of dark) at 21°C. To measure the epidermal cell length and width, 5-d-old dark-grown hypocotyls were incubated in 5 μM FM4-64 dye (Invitrogen) for 10 min. Seven-day-old light-grown roots were incubated in 5 μM FM4-64 dye for 5 min. The apical and basal third of hypocotyls and the root

Downloaded from on November 28, 2017 - Published by www.plantphysiol.org
Copyright © 2014 American Society of Plant Biologists. All rights reserved.

elongation zone were imaged with a 20×/0.25 numerical aperture (NA) objective on a Zeiss Observer Z.1. Wide-field fluorescence micrographs were collected with a charge-coupled device (CCD) camera (QuantEM:512SC; Photometrics). A double-blind experimental design was used for all phenotypic analysis. All image measurements were performed with ImageJ (http://rsb.info.nih.gov/ij/). Data analysis and statistical tests were performed with Microsoft Excel.

VAEM Imaging

VAEM was performed using a total internal reflection fluorescence (TIRF) illuminator on an IX-71 microscope equipped with a 60×/1.45 NA PlanApo TIRF objective (Olympus). YFP-fABD2 was excited with a 488-nm laser line from a solid-state 50-mW laser (Intelligent Imaging Innovations). The emission went through a 525/30-nm filter and was captured with an electron-multiplying CCD camera (ORCA-EM C9100-12; Hamamatsu Photonics). The VAEM platform was operated with Slidebook software (version 5.5.0; Intelligent Imaging Innovations). For the imaging of BDM-treated GFP-fABD2 seedlings, VAEM was performed using a TIRF illuminator on a Zeiss Observer Z.1 equipped with a 100×/1.46 NA PlanApo objective. GFP-fABD2 was excited with a 488-nm laser line from a solid-state 50-mW laser (Intelligent Imaging Innovations). The emission was captured with an electron-multiplying CCD camera (QuantEM:512SC; Photometrics).

Quantitative Analysis of the Architecture of Cortical Actin Arrays

Two parameters, filament abundance (density) and the extent of filament bundling (skewness), were measured as described previously (Higaki et al., 2010; Henty et al., 2011; Li et al., 2012). VAEM snapshots were collected from hypocotyl or root epidermal cells expressing YFP-fABD2 with a fixed laser power, exposure time, and gain setting. Micrographs were cropped and analyzed with ImageJ. At least 150 images of hypocotyl epidermal cells per region, or over 60 images of the root elongation zone from 30 individual seedlings, were collected and analyzed.

Actin Filament Dynamics

VAEM time-lapse series were collected to measure the dynamics of cortical actin arrays in epidermal cells as described previously (Staiger et al., 2009; Henty et al., 2011; Li et al., 2012). Epidermal cells from the apical or basal third of 5-d-old dark-grown hypocotyls or from the root elongation zone of 7-d-old light-grown seedlings were examined. Parameters describing actin turnover and the behavior of filament ends were measured as described (Staiger et al., 2009; Henty et al., 2011; Li et al., 2012). Convolutedness and the rate of change of convolutedness were measured after the actin filament stopped growing. Convolutedness is defined as the ratio of filament length divided by the distance between the plus and minus ends (Smertenko et al., 2010). The rate of change of convolutedness is the average difference in convolutedness between consecutive frames divided by the average time interval between frames. A double-blind experimental design was used to compare the dynamic parameters between genotypes. The time-lapse VAEM images for single filament dynamic measurements were also used for correlation coefficient analyses (Vidali et al., 2010). Images were cropped and analyzed in MATLAB (version 7.14.0, MathWorks) using the method described previously (Vidali et al., 2010).

Supplemental Data

The following materials are available in the online version of this article.

Supplemental Figure S1. Overall actin dynamicity of both single actin filament and actin bundles is reduced in the *xi3KO* mutant.

Supplemental Methods S1. Overall dynamicity analysis for single actin filaments and actin bundles.

ACKNOWLEDGMENTS

We thank Dr. Valerian Dolja (Oregon State University) for kindly providing the *xi3KO* and *xi3KO*;YFP-fABD2 seeds, Benjamin H. Staiger (Purdue University) for customizing the actin architecture and correlation coefficient analysis tools, and Hongbing Luo (Purdue University) for excellent care and maintenance of plant materials. The TIRF microscopy facility was funded in part by the Bindley Bioscience Center, Purdue University.

Received June 2, 2014; accepted September 17, 2014; published September 18, 2014.

LITERATURE CITED

Avisar D, Abu-Abied M, Belausov E, Sadot E, Hawes C, Sparkes IA (2009) A comparative study of the involvement of 17 Arabidopsis myosin family members on the motility of Golgi and other organelles. Plant Physiol **150:** 700–709

Avisar D, Prokhnevsky AI, Makarova KS, Koonin EV, Dolja VV (2008) Myosin XI-K is required for rapid trafficking of Golgi stacks, peroxisomes, and mitochondria in leaf cells of *Nicotiana benthamiana*. Plant Physiol **146:** 1098–1108

Chesarone-Cataldo M, Guérin C, Yu JH, Wedlich-Soldner R, Blanchoin L, Goode BL (2011) The myosin passenger protein Smy1 controls actin cable structure and dynamics by acting as a formin damper. Dev Cell **21:** 217–230

Dyachok J, Zhu L, Liao F, He J, Huq E, Blancaflor EB (2011) SCAR mediates light-induced root elongation in *Arabidopsis* through photoreceptors and proteasomes. Plant Cell **23:** 3610–3626

Funaki K, Nagata A, Akimoto Y, Shimada K, Ito K, Yamamoto K (2004) The motility of *Chara corallina* myosin was inhibited reversibly by 2,3-butanedione monoxime (BDM). Plant Cell Physiol **45:** 1342–1345

Gendreau E, Traas J, Desnos T, Grandjean O, Caboche M, Höfte H (1997) Cellular basis of hypocotyl growth in *Arabidopsis thaliana*. Plant Physiol **114:** 295–305

Henty JL, Bledsoe SW, Khurana P, Meagher RB, Day B, Blanchoin L, Staiger CJ (2011) *Arabidopsis* actin depolymerizing factor4 modulates the stochastic dynamic behavior of actin filaments in the cortical array of epidermal cells. Plant Cell **23:** 3711–3726

Henty-Ridilla JL, Li J, Blanchoin L, Staiger CJ (2013) Actin dynamics in the cortical array of plant cells. Curr Opin Plant Biol **16:** 678–687

Herrmann C, Wray J, Travers F, Barman T (1992) Effect of 2,3-butanedione monoxime on myosin and myofibrillar ATPases. An example of an uncompetitive inhibitor. Biochemistry **31:** 12227–12232

Higaki T, Kutsuna N, Sano T, Kondo N, Hasezawa S (2010) Quantification and cluster analysis of actin cytoskeletal structures in plant cells: role of actin bundling in stomatal movement during diurnal cycles in Arabidopsis guard cells. Plant J **61:** 156–165

Hodge T, Cope MJTV (2000) A myosin family tree. J Cell Sci **113:** 3353–3354

Hussey PJ, Ketelaar T, Deeks MJ (2006) Control of the actin cytoskeleton in plant cell growth. Annu Rev Plant Biol **57:** 109–125

Li J, Arieti R, Staiger CJ (2014a) Actin filament dynamics and their role in plant cell expansion. *In* H Fukuda, ed, Plant Cell Wall Patterning and Cell Shape. John Wiley and Sons, Hoboken, NJ, pp 127–162

Li J, Henty-Ridilla JL, Huang S, Wang X, Blanchoin L, Staiger CJ (2012) Capping protein modulates the dynamic behavior of actin filaments in response to phosphatidic acid in *Arabidopsis*. Plant Cell **24:** 3742–3754

Li J, Staiger BH, Henty-Ridilla JL, Abu-Abied M, Sadot E, Blanchoin L, Staiger CJ (2014b) The availability of filament ends modulates actin stochastic dynamics in live plant cells. Mol Biol Cell **25:** 1263–1275

McCurdy DW (1999) Is 2,3-butanedione monoxime an effective inhibitor of myosin-based activities in plant cells? Protoplasma **209:** 120–125

Murrell MP, Gardel ML (2012) F-actin buckling coordinates contractility and severing in a biomimetic actomyosin cortex. Proc Natl Acad Sci USA **109:** 20820–20825

Nebenführ A, Gallagher LA, Dunahay TG, Frohlick JA, Mazurkiewicz AM, Meehl JB, Staehelin LA (1999) Stop-and-go movements of plant Golgi stacks are mediated by the acto-myosin system. Plant Physiol **121:** 1127–1142

Ojangu EL, Tanner K, Pata P, Järve K, Holweg CL, Truve E, Paves H (2012) Myosins XI-K, XI-1, and XI-2 are required for development of pavement cells, trichomes, and stigmatic papillae in Arabidopsis. BMC Plant Biol **12:** 81

Park E, Nebenführ A (2013) Myosin XIK of *Arabidopsis thaliana* accumulates at the root hair tip and is required for fast root hair growth. PLoS ONE **8:** e76745

Peremyslov VV, Klocko AL, Fowler JE, Dolja VV (2012) Arabidopsis myosin XI-K localizes to the motile endomembrane vesicles associated with F-actin. Front Plant Sci **3:** 184

Downloaded from on November 28, 2017 - Published by www.plantphysiol.org
Copyright © 2014 American Society of Plant Biologists. All rights reserved.

Peremyslov VV, Morgun EA, Kurth EG, Makarova KS, Koonin EV, Dolja VV (2013) Identification of myosin XI receptors in *Arabidopsis* defines a distinct class of transport vesicles. Plant Cell **25:** 3022–3038

Peremyslov VV, Prokhnevsky AI, Avisar D, Dolja VV (2008) Two class XI myosins function in organelle trafficking and root hair development in Arabidopsis. Plant Physiol **146:** 1109–1116

Peremyslov VV, Prokhnevsky AI, Dolja VV (2010) Class XI myosins are required for development, cell expansion, and F-Actin organization in *Arabidopsis*. Plant Cell **22:** 1883–1897

Prokhnevsky AI, Peremyslov VV, Dolja VV (2008) Overlapping functions of the four class XI myosins in Arabidopsis growth, root hair elongation, and organelle motility. Proc Natl Acad Sci USA **105:** 19744–19749

Šamaj J, Peters M, Volkmann D, Baluška F (2000) Effects of myosin ATPase inhibitor 2,3-butanedione 2-monoxime on distributions of myosins, F-actin, microtubules, and cortical endoplasmic reticulum in maize root apices. Plant Cell Physiol **41:** 571–582

Sampathkumar A, Gutierrez R, McFarlane HE, Bringmann M, Lindeboom J, Emons AM, Samuels L, Ketelaar T, Ehrhardt DW, Persson S (2013) Patterning and lifetime of plasma membrane-localized cellulose synthase is dependent on actin organization in Arabidopsis interphase cells. Plant Physiol **162:** 675–688

Schuh M (2011) An actin-dependent mechanism for long-range vesicle transport. Nat Cell Biol **13:** 1431–1436

Smertenko AP, Deeks MJ, Hussey PJ (2010) Strategies of actin reorganisation in plant cells. J Cell Sci **123:** 3019–3028

Smith LG, Oppenheimer DG (2005) Spatial control of cell expansion by the plant cytoskeleton. Annu Rev Cell Dev Biol **21:** 271–295

Sparkes IA, Teanby NA, Hawes C (2008) Truncated myosin XI tail fusions inhibit peroxisome, Golgi, and mitochondrial movement in tobacco leaf epidermal cells: a genetic tool for the next generation. J Exp Bot **59:** 2499–2512

Staiger CJ, Sheahan MB, Khurana P, Wang X, McCurdy DW, Blanchoin L (2009) Actin filament dynamics are dominated by rapid growth and severing activity in the Arabidopsis cortical array. J Cell Biol **184:** 269–280

Szymanski DB, Cosgrove DJ (2009) Dynamic coordination of cytoskeletal and cell wall systems during plant cell morphogenesis. Curr Biol **19:** R800–R811

Tominaga M, Kimura A, Yokota E, Haraguchi T, Shimmen T, Yamamoto K, Nakano A, Ito K (2013) Cytoplasmic streaming velocity as a plant size determinant. Dev Cell **27:** 345–352

Tominaga M, Yokota E, Sonobe S, Shimmen T (2000) Mechanism of inhibition of cytoplasmic streaming by a myosin inhibitor, 2,3-butanedione monoxime. Protoplasma **213:** 46–54

Ueda H, Yokota E, Kutsuna N, Shimada T, Tamura K, Shimmen T, Hasezawa S, Dolja VV, Hara-Nishimura I (2010) Myosin-dependent endoplasmic reticulum motility and F-actin organization in plant cells. Proc Natl Acad Sci USA **107:** 6894–6899

Vidali L, Burkart GM, Augustine RC, Kerdavid E, Tüzel E, Bezanilla M (2010) Myosin XI is essential for tip growth in *Physcomitrella patens*. Plant Cell **22:** 1868–1882

Vidali L, Rounds CM, Hepler PK, Bezanilla M (2009) Lifeact-mEGFP reveals a dynamic apical F-actin network in tip growing plant cells. PLoS ONE **4:** e5744

Vogel SK, Petrasek Z, Heinemann F, Schwille P (2013) Myosin motors fragment and compact membrane-bound actin filaments. eLife **2:** e00116

Yu JH, Crevenna AH, Bettenbühl M, Freisinger T, Wedlich-Söldner R (2011) Cortical actin dynamics driven by formins and myosin V. J Cell Sci **124:** 1533–1541

Zheng M, Beck M, Müller J, Chen T, Wang X, Wang F, Wang Q, Wang Y, Baluška F, Logan DC, et al (2009) Actin turnover is required for myosin-dependent mitochondrial movements in Arabidopsis root hairs. PLoS ONE **4:** e5961

Downloaded from on November 28, 2017 - Published by www.plantphysiol.org
Copyright © 2014 American Society of Plant Biologists. All rights reserved.